blood®
Regular Article

LYMPHOID NEOPLASIA

14q32 rearrangements deregulating *BCL11B* mark a distinct subgroup of T-lymphoid and myeloid immature acute leukemia

Danika Di Giacomo,[1,*] Roberta La Starza,[1,*] Paolo Gorello,[1] Fabrizia Pellanera,[1] Zeynep Kalender Atak,[2] Kim De Keersmaecker,[3] Valentina Pierini,[1] Christine J. Harrison,[4] Silvia Arniani,[1] Martina Moretti,[1] Nicoletta Testoni,[5] Giovanna De Santis,[6] Giovanni Roti,[7] Caterina Matteucci,[1] Renato Bassan,[8] Peter Vandenberghe,[9] Stein Aerts,[10] Jan Cools,[11] Beat Bornhauser,[12] Jean-Pierre Bourquin,[12] Rocco Piazza,[13] and Cristina Mecucci[1]

[1]Department of Medicine and Surgery, University of Perugia, Perugia, Italy; [2]Cancer Research UK Cambridge Institute, University of Cambridge, Cambridge, United Kingdom; [3]KU Leuven and Leuven Cancer Institute, Leuven, Belgium; [4]Translational and Clinical Research Institute, Newcastle University Centre for Cancer, Newcastle-upon-Tyne, United Kingdom; [5]"Seràgnoli" Institute, University of Bologna, Bologna, Italy; [6]UOC of Hematology, Avellino, Italy; [7]Department of Medicine and Surgery, University of Parma, Parma, Italy; [8]Ospedale dell'Angelo, Venice, Italy; [9]University Hospital Leuven, Leuven, Belgium; [10]VIB Center for Brain & Disease Research, Leuven, Belgium;[11]KU Leuven-VIB, Leuven, Belgium; [12]University Children's Hospital, Zurich, Switzerland; and [13]Department of Medicine and Surgery, University of Milano-Bicocca, Monza, Italy

KEY POINTS

- **14q32 rearrangements, activating *BCL11B*, provide a novel biomarker for a new entity among immature acute leukemias.**

Acute leukemias (ALs) of ambiguous lineage are a heterogeneous group of high-risk leukemias characterized by coexpression of myeloid and lymphoid markers. In this study, we identified a distinct subgroup of immature acute leukemias characterized by a broadly variable phenotype, covering acute myeloid leukemia (AML, M0 or M1), T/myeloid mixed-phenotype acute leukemia (T/M MPAL), and early T-cell precursor acute lymphoblastic leukemia (ETP-ALL). Rearrangements at 14q32/*BCL11B* are the cytogenetic hallmark of this entity. In our screening of 915 hematological malignancies, there were 202 AML and 333 T-cell acute lymphoblastic leukemias (T-ALL: 58, ETP; 178, non-ETP; 8, T/M MPAL; 89, not otherwise specified). We identified 20 cases of immature leukemias (4% of AML and 3.6% of T-ALL), harboring 4 types of 14q32/*BCL11B* translocations: t(2,14)(q22.3;q32) (n = 7), t(6;14)(q25.3;q32) (n = 9), t(7;14)(q21.2;q32) (n = 2), and t(8;14)(q24.2;q32) (n = 2). The t(2;14) produced a *ZEB2-BCL11B* fusion transcript, whereas the other 3 rearrangements displaced transcriptionally active enhancer sequences close to *BCL11B* without producing fusion genes. All translocations resulted in the activation of *BCL11B*, a regulator of T-cell differentiation associated with transcriptional corepressor complexes in mammalian cells. The expression of *BCL11B* behaved as a disease biomarker that was present at diagnosis, but not in remission. Deregulation of *BCL11B* co-occurred with variants at *FLT3* and at epigenetic modulators, most frequently the *DNMT3A*, *TET2*, and/or *WT1* genes. Transcriptome analysis identified a specific expression signature, with significant downregulation of BCL11B targets, and clearly separating *BCL11B* AL from AML, T-ALL, and ETP-ALL. Remarkably, an ex vivo drug-sensitivity profile identified a panel of compounds with effective antileukemic activity.

Introduction

The current World Health Organization (WHO) classification of acute leukemia (AL) has been guided by molecular-cytogenetic entities and their clinical impact. Recurrent molecular-cytogenetic rearrangements serve as both diagnostic markers and as independent prognostic factors for risk group assignment and treatment choice. However, heterogeneous subgroups of leukemia are lacking genetic characterization, with no clear evidence of differentiation into a single lineage. In addition, some have variable combinations of myeloid and T- or B-cell components (mixed phenotypes). These leukemias, defined by the WHO classification as acute leukemias of ambiguous lineage (ALALs), include acute undifferentiated leukemia, acute leukemias with ambiguous lineage, and mixed-phenotype acute leukemias (MPALs).[1] So far, only 2 cytogenetic markers [t(9;22)(q34;q22)/*BCR-ABL1* and *KMT2A* rearrangements], mainly associated with B/myeloid MPAL, have been incorporated to improve diagnosis and risk stratification.[1] Notably, 2 recent studies have begun to elucidate the genetic basis of pediatric ALAL, and adult MPAL, identifying recurrent genetic and/or epigenetic events that overlap with those found in acute myeloid leukemia (AML) and B- or T-cell acute lymphoblastic leukemia (ALL).[2,3]

An additional WHO entity, termed early T-cell precursor ALL (ETP-ALL), is a subgroup of high-risk T-ALLs[4,5] with very immature T progenitors that retain myeloid differentiation potential.[6] ETP-ALL cases lack a unifying cytogenetic marker.[7]

In this study, we focused on 14q32 rearrangements involving *BCL11B*, a transcription factor interacting with the nucleosome remodeling and deacetylase (NuRD) complex,[8,9] which is essential for T-cell development and for maintenance of T-cell identity.[10,11] We found that 14q32 rearrangements that activate *BCL11B* are the hallmark of a leukemia entity, referred to herein as *BCL11B*-a (activated) AL, and characterized by expression of both myeloid and T-lymphoid antigens with a distinct transcriptomic profile.

Methods

Patients

Patients were recruited from the Hematology Departments, at the Universities of Perugia, Parma, and Bologna, Italy; Venezia-Mestre and Avellino Hospitals, Italy; the Centre for Human Genetics, University of Leuven, Belgium; and the Leukemia Research Cytogenetics Group, Translational and Clinical Research Institute Newcastle University Centre for Cancer, United Kingdom. All patients or their parents/guardians provided informed consent for sample collection and its use in approved research studies. This study was approved by the local bioethics committee (Bioethics Committees: University of Perugia, number 2014-0259; University of Leuven, number S53745; University Centre for Cancer, Newcastle-upon-Tyne, number 2007-004013-34; and Bioethics Committee of the Canton of Zurich, number 2014-0383). Molecular analyses were performed in agreement with the Declaration of Helsinki.

Cytogenetics, fluorescence in situ hybridization, reverse transcription polymerase chain reaction, and single-nucleotide polymorphism array

Conventional cytogenetic analysis was performed after G banding (supplemental Material, available on the *Blood* Web site). Fluorescence in situ hybridization (FISH) testing was performed to refine the 14q32 breakpoints and the breakpoints of chromosome partners, by using the DNA clones listed in supplemental Table 1. Reverse transcription polymerase chain reaction (RT-PCR) and western blot analysis were performed according to standard procedures (supplemental Material). Single-nucleotide polymorphism array (SNPa) analysis determined copy number variants (CNVs) and copy-neutral loss of heterozygosity (cnLOH; supplemental Material).

Quantitative RT-PCR

Quantitative RT-PCR was used to assess the expression of *BCL11B*, *SPI1*/PU.1, and *ZEB2*. Details are provided in the supplemental Material.

RNA sequencing

RNA sequencing (RNA-Seq) experiments are described in the supplemental Material. AML[12] and T-ALL[13] series, which were used as references, belong to the cBioPortal data sets[14,15] (The Cancer Genome Atlas [TCGA] for AML and TARGET for T-ALL projects) and GDC Data Portal data sets[16] (projects TCGA-LAML for AML and TARGET-ALL-P2 for T-ALL). Normalized counts from all *BCL11B*-a AL samples were used for differential expression and Gene Set Enrichment Analyses. See the supplemental Material for details.

Targeted sequencing and whole-exome sequencing

Gene variants were investigated by targeted sequencing with the Myeloid Solution SOPHiA Genetics (Saint-Sulpice, Switzerland), which covers 30 relevant genes associated with myeloid hemopathies, and/or by whole-exome sequencing (supplemental Material). Sanger sequencing was used to validate next-generation sequencing (NGS) findings and to study hot-spot mutations in selected cases. Detailed procedures and analyses of the data are provided in the supplemental Material.

Drug sensitivity and resistance profiling

We tested 65 clinical and preclinical compounds on 5 *BCL11B*-a AL samples with available material [case 4 with t(2;14); cases 9, 10, and 12 with t(6;14); and case 18 with t(7;14); Table 1] and compared drug sensitivity with that in 23 cases of T-ALL.[17] Primary cells were recovered from cryopreserved bone marrow aspirates. Drug responses were assessed in leukemia cells cocultured on hTERT-immortalized primary human bone marrow mesenchymal stromal cells, as previously described.[17] Detailed procedures are provided in the supplemental Material.

Results

Identification and molecular characterization of 4 recurrent 14q32/*BCL11B* translocations

We collected 915 cases with lymphoid and myeloid malignant hemopathies (supplemental Table 2). They included 96 cases of chronic lymphocytic leukemia, 76 of multiple myeloma, 96 of myelodysplastic syndrome, and 647 of acute leukemia. Of the acute leukemias, 29 were acute promyelocytic leukemia, 83 B-ALL, 202 AML (supplemental Table 3), and 333 T-ALL (178, non-ETP-ALL; 58, ETP-ALL; 8, T/M MPAL; and 89, not otherwise specified).

FISH screening for *BCL11B*, which is oriented from telomere to centromere and maps centromeric to the *IGH* locus, detected known *BCL11B* rearrangements in T-ALL: t(5;14)(q35;q32)/*BCL11B-TLX3* (n = 45), t(5;14)(q34;q32)/*BCL11B-NKX2.5* (n = 1), t(7;14)(p15;q32)/*BCL11B-HOXA* (n = 1), and inv(14)(q13q32)/*BCL11B-NKX2-1* (n = 1). In addition, we found 20 cases (8 of 202 AML [4%], M0 or M1 subtype, and 12 of 333 T-ALL [3.6%], including 7 ETP-ALL, 3 T/M MPAL, and 2 T-ALL not otherwise specified) with more telomeric clusters of breakpoints at 14q32/*BCL11B* (Figure 1A; Table 1; supplemental Table 4) that were all specifically identified by fosmids WI2-2168J13 and WI2-2934J16 (supplemental Figures 1A, 2A, 3A, and 4A). The immunophenotype, available in 18 of 20 cases, showed an immature phenotype in both AML (8 of 8) and T-ALL (10 of 10).

Overall, there were 4 translocations: t(7;14)(q21.2;q32) (n = 2) (supplemental Figure 1A); t(2;14)(q22.3;q32) (n = 7; supplemental Figure 2A); t(6;14)(q25.3;q32) (n = 9; supplemental Figure 3A); and t(8;14)(q24.2;q32) (n = 2; supplemental Figure 4A).

Molecular characterization of t(7;14)(q21.2;q32) In the 2 cases with t(7;14)(q21.2;q32), the 14q32 breakpoints were narrowed between fosmids WI2-2168J13 and WI2-1945I12, an 85-kb region downstream of *BCL11B* (Figure 1A). The 7q21.2 breakpoints fell within *CDK6* (Figure 1B). In both cases, the full

Table 1. Details of *BCL11B*-a AL cases

Case	Code	Sex/age, y	FAB/WHO diagnosis	Immunophenotype	Karyotype
t(2;14)(q22;q32)					
1	UPN#455	M/72	AML	NA	46,XY,**t(2;14)(q22;q32)**[4]/46,XY[9]
2	UPN#456	M/52	T/myeloid MPAL	**CD2$^+$, CD117$^+$, CD34$^+$, HLA-DR$^+$, CD13$^+$**, TdT$^+$, cCD3$^+$, CD56$^+$, MPO$^+$, cCD79a$^+$, CD7$^-$, CD3$^-$, CD5$^-$, CD33$^-$, CD14$^-$, CD15$^-$, CD22$^-$, CD20$^-$	46,XY,**t(2;14)(q22;q32)**[19]/47,idem,+4[3]
3	UPN#457	M/37	AML M0	**CD2$^+$, CD117$^+$, CD34$^+$, HLA-DR$^+$, CD13$^+$**, TdT$^+$, CD7$^+$, CD15$^+$, MPO$^{+/-}$, CD33$^{+/-}$, CD14$^-$, CD11c$^-$, CD3$^-$, CD4$^-$, CD8$^-$, CD5$^-$, CD10$^-$, CD19$^-$	46,XY,**t(2;14)(q22;q32)**[15]
4	UPN#141	F/76	AML M0	**CD2$^+$, CD117$^+$, CD34$^+$, HLA-DR$^+$, CD13$^+$**, CD7$^+$, MPO$^+$, CD11b$^+$, CD38$^+$, CD33$^-$, CD14$^-$, CD15$^-$, cCD3$^-$, CD3$^-$, CD4$^-$, CD56$^-$, CD10$^-$, cCD79a$^-$, CD19$^-$	46,XX,**t(2;14)(q22;q32)**,del(5)(q13q31)[15]
5	UPN#458	F/68	AML M1	**CD2$^+$, CD117$^+$, CD34$^+$, HLA-DR$^+$, CD13$^+$**, CD7$^+$, MPO$^{+/-}$, CD33$^+$, CD14$^-$, TdT$^-$, CD3$^-$, CD4$^-$, CD8$^-$, CD1a$^-$, CD10$^-$, CD19$^-$, CD22$^-$	46,XX,**t(2;14)(q22;q32)**[12]/46,idem,add(12)(q24)[5]/46,XX[3]
6	UPN#151	M/18	AML M1	**CD2$^+$, CD117$^+$, CD34$^+$, HLA-DR$^+$, CD13$^+$**, CD15$^+$, CD56$^+$, MPO$^-$, CD33$^-$, CD14$^-$, CD7$^-$, cCD3$^-$, CD3$^-$, CD4$^-$, CD5$^-$, CD19$^-$, cCD79a$^-$	46,XY,**t(2;14)(q22;q32)**,del(16)(q21)[15]
7	UPN#459	M/64	ETP-ALL	**CD2$^+$, CD117$^+$, CD34$^+$, HLA-DR$^+$, CD13$^+$,** CD11b$^+$, CD56$^+$, TdT$^+$, CD7$^+$, CD38$^+$, cCD3$^+$, MPO$^-$, CD33$^-$, CD4$^-$, CD5$^-$, CD1a$^-$, CD10$^-$, CD19$^-$, CD20$^-$, cCD79a$^-$	46,XY[24].**ish t(2;14)(q22;q32)(WI2-2194I13+;WI2-2001J18+)**[5]
t(6;14)(q25;q32)					
8	UPN#143	M/17	AML-M1	**CD2$^+$, CD117$^+$, CD34$^+$, HLA-DR$^+$, CD13$^+$**, TdT$^+$, CD33$^+$, MPO$^+$, CD56$^+$, CD15$^+$, CD14$^-$, CD7$^-$, cCD3$^-$, CD3$^-$, CD4$^-$, CD5$^-$, CD10$^-$, CD19$^-$, CD20$^-$, cCD79a$^-$	46,XY,**t(6;14)(q25;q32)**[15]
9	UPN#145	M/59	T/myeloid MPAL	**CD2$^+$, CD117$^+$, CD34$^+$, CD13$^+$**, CD7$^+$, TdT$^+$, cCD3$^+$, CD3$^-$, CD8$^-$, CD4$^-$, CD5$^-$, CD1a$^-$, CD10$^-$, cCD79a$^-$, **CD2$^+$, CD13$^+$, CD33$^+$**, CD11b$^+$, MPO$^+$, CD14$^+$, CD34$^-$, CD117$^-$, CD10$^-$, cCD79a$^-$	46,XY,**t(6;14)(q25;q32)**,del(11)(p13p15)[15]
10	UPN#460	M/48	ETP-ALL	**CD2$^+$, CD117$^+$, CD34$^+$, HLA-DR$^+$, CD13$^+$**, CD7$^+$, TdT$^+$, CD33$^+$, CD38$^+$, CD45$^+$, CD99$^+$, CD133$^+$, cCD3$^+$, CD3$^-$, CD4$^-$, CD5$^-$, CD8$^-$, CD52$^-$, CD56$^-$, CD65$^-$, CD79a$^-$, MPO$^-$, TCR A/B$^-$, TCR G/D$^-$, CD10$^-$, CD19$^-$, cCD79a$^-$	46,XY,add(19)(q13)[10]/46,XY[5].**ish ins(6;14)(q25;q32q32)(WI2-2194I13+;WI2-2934J16+)**[6]
11	UPN#260	M/4	ETP-ALL	**CD2$^+$, CD117$^+$, CD34$^+$, HLA-DR$^+$, CD33$^+$,** CD7$^+$, TdT$^+$, CD38$^+$, CD45$^+$, cCD3$^+$, CD11b$^+$, MPO$^{+/-}$, CD99$^+$, CD3$^-$, CD4$^-$, CD5$^-$, CD8$^-$, CD1a$^-$, CD56$^-$, CD13$^-$, CD14$^-$, CD14$^-$, CD65$^-$, CD10$^-$, CD19$^-$	46,XY[10].**ish t(6;14)(q25;q32)(WI2-2194I13+;WI2-2001J18+)**[5]

Positive antigens common to all cases with available immunophenotype and the 14q32/*BCL11B* translocation are indicated in bold.
NA, not available.

Table 1. (Continued)

Case	Code	Sex/age, y	FAB/WHO diagnosis	Immunophenotype	Karyotype
12	UPN#462	F/78	ETP-ALL	**CD2$^+$, CD117$^+$, CD34$^+$, HLA-DR$^+$, CD13$^+$,** CD7$^+$, CD38$^+$, cCD3$^+$, TdT$^-$, CD4$^-$, CD8$^-$, CD3$^-$, CD5$^-$, CD56$^-$, CD79a$^-$, CD15$^-$, CD33$^-$, MPO$^-$, CD61$^-$, CD10$^-$, CD19$^-$, CD20$^-$, CD22$^-$, cCD79a$^-$	47,XX,+4[8]/46,XX[8].**nuc ish(WI2-2001J18X2),(WI2-2194I13X2),(WI2-2001J18 sep WI2-2194I13X1)** [70/100]
13	UPN#463	M/18	T-ALL unspecified	NA	47,XY,+4[15]/46,XY[15].**ish t(6;14)(q25;q32)(WI2-2194I13+; WI2-2001J18+)**[3]
14	UPN#464	M/29	T-ALL unspecified	NA	**nuc ish(WI2-2001J18X2),(WI2-2194I13X2),(WI2-2001J18 sep WI2-2194I13X1)**[70/106]
15	UPN#465	M/12	ETP-ALL	NA	46,XY,**t(6;14)(q25;q32),**del(12)(p11p13)[9]/46,XY[6]
16	UPN#466	M/44	ETP-ALL	**CD2$^+$, CD117$^+$, CD34$^+$, HLA-DR$^+$, CD13$^+$,** CD7$^+$, CD38$^+$, TdT$^+$, CD33$^-$, sCD3$^-$, CD4$^-$, CD8$^-$, CD5$^-$, CD56$^-$, CD10$^-$, CD19$^-$	46,XY,**t(6;14)(q25;q32)** [9]/46,XY[3]
t(7;14)(q22;q32)					
17	UPN#149	M/51	ETP-ALL	**CD2$^+$, CD117$^+$, CD34$^+$, HLA-DR$^{+/-}$,** cCD3$^+$, TdT$^+$, CD7$^{+/-}$, CD15$^{+/-}$, sCD3$^-$, CD5$^-$, CD4$^-$, CD8$^-$, MPO$^-$, CD13$^-$, CD33$^-$, CD10$^-$, cCD79a$^-$	46,XY,**t(7;14)(q21;q32)** [16]/46,XY[5]
18	UPN#147	M/50	T/myeloid MPAL	**CD2$^+$, CD117$^+$, CD34$^+$, HLA-DR$^+$,** CD7$^+$, CD38$^+$, CD15$^+$, **CD3$^+$, CD2$^+$, CD117$^+$, CD34$^+$, HLA-DR$^+$, CD33dim, CD13dim,** CD7$^+$, CD38$^+$, CD15$^+$, MPO$^+$, CD36$^+$, CD123$^+$, CD10$^-$, CD19$^-$, CD22$^-$, cCD79a$^-$	46,XY,**t(7;14)(q21;q32)** [9]/46,XY[1]
t(8;14)(q24;q32)					
19	UPN#461	M/65	AML M0	**CD2$^+$, CD117$^+$, CD34$^+$, HLA-DR$^{+/-}$, CD13$^+$,** CD7$^+$, cCD3$^-$, CD3$^-$, CD4$^-$, CD1a$^-$, CD5$^-$, CD8$^-$, MPO$^-$, TdT$^-$, CD10$^-$, CD19$^-$	46,XY,t(2;5)(p21;q13)[10]/46,XX[9].**nuc ish(WI2-2194I13X2),(WI2-2934J16X2),(WI2-2194I13 sep WI2-2934J16)[100/120]**
20	UPN#467	M/51	AML M0	**CD2$^+$, CD117$^+$, CD34$^+$, HLA-DR$^+$, CD13$^+$,** CD7$^+$, MPO$^-$, CD33$^-$, cCD3$^-$, CD3$^-$, CD8$^-$, CD5$^-$, CD56$^-$, CD19$^-$, cCD79a$^-$	46,XY[10].**nuc ish(WI2-2194I13X2),(WI2-2934J16X2),(WI2-2194I13 sep WI2-2934J16)**[91/100]

Positive antigens common to all cases with available immunophenotype and the 14q32/*BCL11B* translocation are indicated in bold.
NA, not available.

length of *BCL11B* moved to der(7), at the 3' end of *CDK6* (supplemental Material).

Molecular characterization of t(2;14)(q22.3;q32) In the 7 cases with t(2;14)(q22.3;q32), the 14q32 breakpoints fell between fosmids WI2-2001J18 and WI2-2194I13 (Figure 1A), whereas the 2q22.3 breakpoints mapped within the zinc finger E-box binding homeobox 2 (*ZEB2*) gene (Figure 1C). By cloning and sequencing, we found an in-frame *ZEB2-BCL11B* fusion transcript in all cases. Whereas breakpoints in *ZEB2* were alternatively located in exon 2 or 4 (NM_ 014795.3), the breakpoint in *BCL11B* invariably fell in exon 2 (nucleotide 554; NM_138576.3; supplemental Figure 2B). Therefore, regulation of *BCL11B* transcription moved under the control of the *ZEB2* promoter. The predicted ZEB2-BCL11B proteins retained all the BCL11B functional domains (supplemental Figure 2C-D).

Molecular characterization of t(6;14)(q25.3;q32) Rearrangements between 6q25.3 and 14q32 consisted of a balanced t(6;14)(q25.3;q32) (n = 8) or an ins(6;14)(q25.3;q32q32) (n = 1) (Table 1). The 14q32 breakpoints were slightly variable and localized between fosmids WI2-2001J18 and WI2-2934J16 (Figure 1A). The 6q25 breakpoints were detected by clone RP11-19F10 (7 cases) or clone RP11-446N2 (2 cases) in a region of ~100-kb without known genes (Figure 1D). In all cases, rearrangements did not produce fusion transcripts but relocated *ARID1B* and its regulatory sequences closes to *BCL11B* at der(6) (case 10) or der(14) (cases 8, 9, and 11-16; Figure 1D).[18,19]

Molecular characterization of t(8;14)(q24.2;q32) In the 2 cases with t(8;14)(q24.2;q32), the 14q32 breakpoints, upstream of *BCL11B*, mapped between fosmids WI2-2194I13 and WI2-2934J16 (Figure 1A), whereas the 8q24.2 breakpoints, telomeric

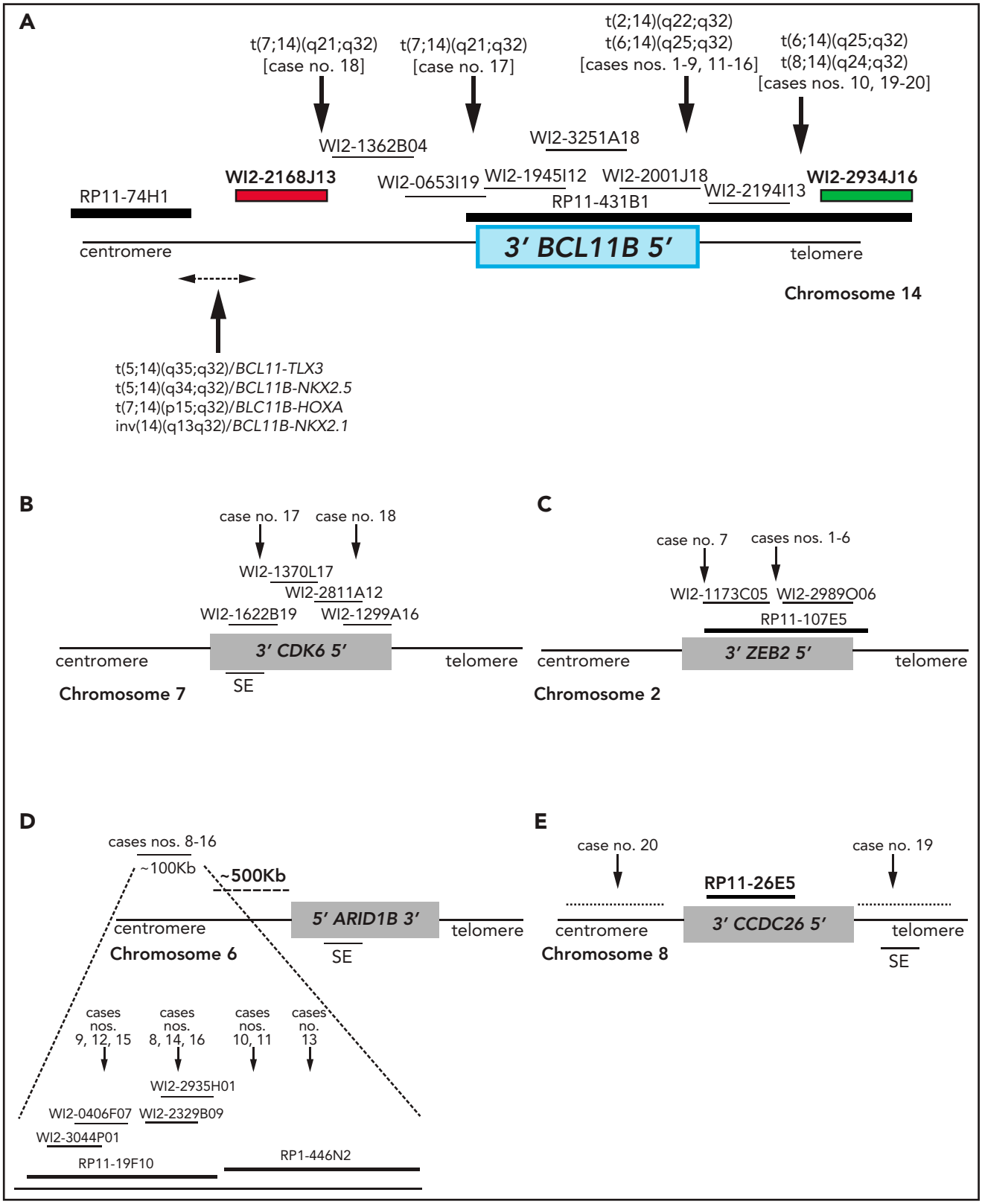

Figure 1. Breakpoint characterization in *BCL11B*-a AL. (A) Break-apart FISH assay differentiating t(2;14), t(6;14), t(7;14), and t(8;14) translocations (fosmid WI2-2168J13, red and fosmid WI2-2934J16, green) from 4 known rearrangements in T-ALL. The thin black horizontal lines represent fosmids that were used to narrow the 14q32 breakpoints. Arrows indicate the mapping of the breakpoint in each case. (B-E) Mapping of breakpoints at *CDK6*/7q21.2 (B); *ZEB2*/2q22.3 (C); 6q25.3 (D); 8q24 (E). Patient case numbers refer to Table 1. The figure panels are not to scale. SE, superenhancer.

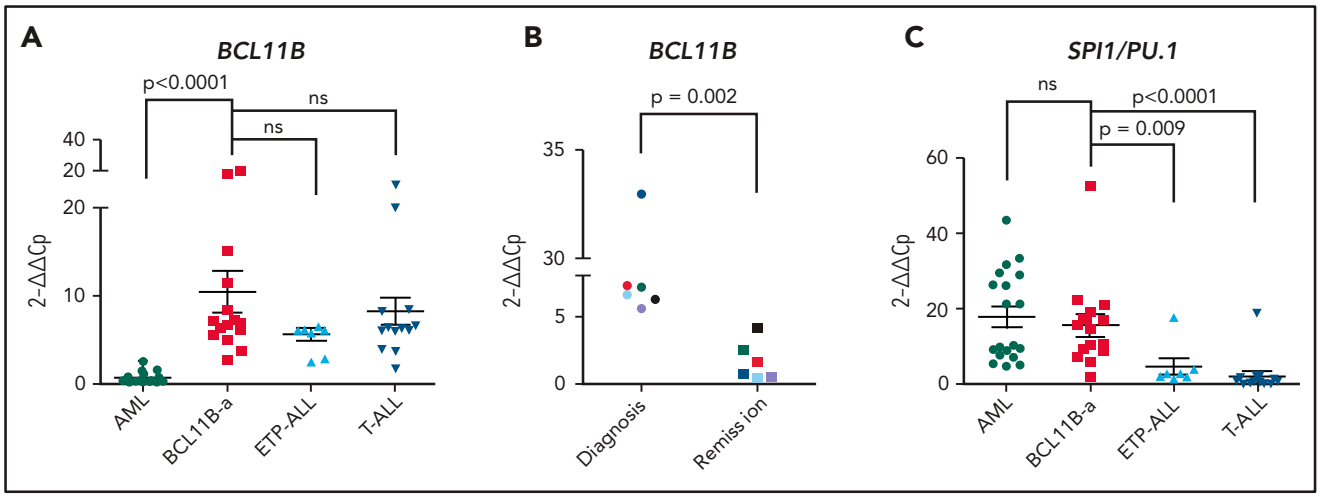

Figure 2. 14q32 rearrangements result in the activation of *BCL11B* and *SPI1*/PU.1. (A) Expression of *BCL11B* in 15 *BCL11B*-a AL cases (1-4, 6-13, 17-18, and 20; Table 1) compared with in-house series of AML (n = 19), ETP-ALL (n = 8), and T-ALL (n = 15) cases. (B) One of 3 independent experiments showing longitudinal expression of *BCL11B* in 6 paired diagnosis-remission *BCL11B*-a AL cases: case 4 (black), case 6 (blue), case 8 (red), case 9 (green), case 17 (light blue), and case 18 (violet). Patient case numbers refer to Table 1. (C) Expression of *SPI1*/PU.1 in 15 *BCL11B*-a cases (1-4, 6-13, 17-18, 20; Table 1) compared with in-house series of AML (n = 19), ETP-ALL (n = 7), and T-ALL (n = 15) cases. Values are expressed as means ± standard error of the mean. Cp, crossing point; ns, not significant.

to *MYC*, were narrowed by clone RP11-26E5, which maps ~50 kb centromeric to the BENC enhancer region and encompasses *CCDC26*. This clone was retained on der(8) in case 19, whereas it moved to der(14) in case 20 (Figure 1E; supplemental Material).

Karyotype was available in 19 of 20 cases (Table 1) and 14q32/*BCL11B* translocations were detected in 12 cases. In 9 of them, the translocation was the only chromosomal change (Table 1). SNPa results were available in 15 of 20 cases and confirmed a low burden of co-occurring abnormalities (mean, 1.6; range, 0-6; supplemental Table 5). Additional chromosomal abnormalities (ACAs) included trisomy 4 in 3 cases (2, 12, and 13; Table 1), a 16q deletion encompassing *CTCF* gene in 2 cases (6 and 17; Table 1), and a del(5q) in 1 case (4; Table 1). Notably, a 4q trisomy has been reported in immature T-ALL by Takahashi et al,[3] and the interstitial deletion of 5q is a recurrent CNV described in ETP-ALL by our group.[20] Moreover, common cnLOHs were found at 2p25.3-p24.1 and 2p22.3-p13.2 (cases 2 and 19) and at 9p24.3-p21 (cases 9 and 20).

Clinical and phenotypic features of *BCL11B*-a AL

BCL11B-a AL cases showed male predominance (M/F: 17/3) and a median age of 50.5 years (range, 4-78) (Table 1). Immunophenotypic characterization was available in 16 cases, all of which shared an immature immunophenotype characterized by expression of the hematopoietic stem cell markers HLA-DR, CD117, and/or CD34. All cases shared positivity for the T-lineage surface marker CD2. Fifteen cases were positive for myeloid antigens CD13 and/or CD33; MPO was positive or weak in 8 cases. Positivity for CD7 and cCD3 was found in 13 and 8 cases, respectively. More mature T-lineage antigens, such as CD1a, CD5, and CD8, were always absent (Table 1).

Overlapping features emerged in 6 cases in which morphological revision of May-Grunwald-Giemsa–stained bone marrow smears was performed. Blasts were variable in size, with a high nuclear/cytoplasmic ratio and an agranular cytoplasm. In variable percentages (20% to 90%), kidney-shaped nuclei with invagination/indentation, prominent nucleoli, and some hand mirror cells were observed (supplemental Figure 5).

14q32 rearrangements result in *BCL11B* activation

In *BCL11B*-a AL cases, *BCL11B* was activated, showing a significant upregulation compared with AML ($P < .0001$) and similar levels of expression compared with cases of T-ALL and ETP-ALL (Figure 2A). Activation was found at diagnosis, but not at hematological and cytogenetic remission (Figure 2B). Moreover, in the t(2;14)-associated *BCL11B*-a AL, a specific test showed low expression of the wild-type *BCL11B*, indicating that upregulation involved only the fusion transcript (supplemental Figure 6A-B). Whether overexpression was related to 1 or both alleles in all the other *BCL11B*-a ALs could not be determined.

It is worth noting that, in the thymus, *BCL11B* and *SPI1*/PU.1 show an inverse modulation during T-lineage commitment.[11,21]; *SPI1*/PU.1 expression declines, whereas the *BCL11B* gene switches on and progressively increases. Thus, we investigated *SPI1*/PU.1 levels in our cohort of patients and found that it was significantly higher in *BCL11B*-a AL than in ETP-ALL ($P = .009$) and non-ETP T-ALL ($P < .0001$), whereas no differences emerged in the comparison with AML (Figure 2C). We also investigated the expression of *ZEB2*, which was rearranged in cases with the t(2;14) translocation. *BCL11B*-a AL showed a significant overexpression of *ZEB2* when compared with T-ALL ($P < .0001$) and ETP-ALL ($P = .009$), but not when compared with AML (supplemental Figure 7A). Likewise, the single case of t(2;14)/*ZEB2-BCL11B* described by Goossens et al belonged to the immature subgroup of T-ALL, which showed a significantly higher expression of *ZEB2* than the more mature T-ALLs.[22] Moreover, we found a similar *ZEB2* expression at both diagnosis and remission (supplemental Figure 7B). This finding may be explained by *ZEB2* expression in the normal myeloid compartment.[23]

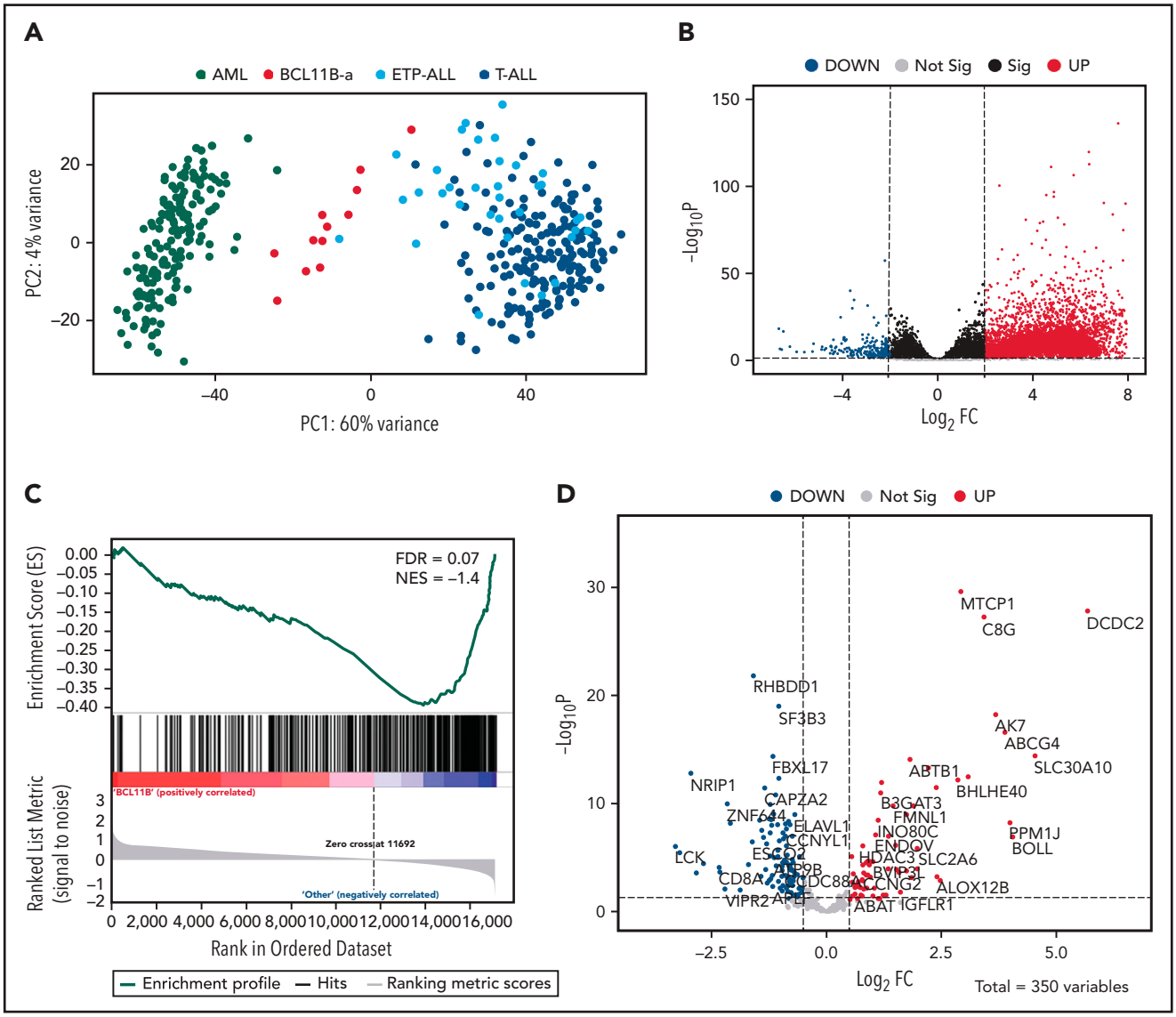

Figure 3. Distinct expression profile in *BCL11B*-a AL. (A) Scatter plot showing variance distribution of *BCL11B*-a AL, AML, ETP-ALL, and T-ALL cases emphasized by principal component analysis 1 (PC1). (B) Volcano plot showing the gene expression in *BCL11B*-a AL cases compared with AML, ETP-ALL, and T-ALL. Log_2FC is plotted against the $-Log_{10}$-adjusted *P* value. Black indicates genes with a significant FDR (≦0.05). Red and blue represent upregulated and downregulated differentially expressed genes, respectively (FDR ≦ 0.05, $|Log_2 FC| \geq 2$). Gray, nonsignificantly expressed genes. (C) Gene set enrichment analysis of BCL11B target genes in *BCL11B*-a AL cases vs other leukemic groups (AML, ETP-ALL, and T-ALL). (D) Volcano plot showing the distribution of 350 BCL11B targets in *BCL11B*-a AL cases compared with other leukemias. Log_2FC is plotted against the $-Log_{10}$-adjusted *P* value. Red and blue represent significant (FDR ≦0.05) upregulated and downregulated targets, respectively; NES, normalized enrichment score; FC, fold change.

A distinct expression profile marks *BCL11B*-a AL cases

Unsupervised analysis of normalized counts obtained from RNA-seq separated *BCL11B*-a AL from T-ALL, ETP-ALL, and AML in the first principal component, showing a total variance of 60% (Figure 3A). Differential expression analysis identified 5144 deregulated genes. Upregulation (4852 upregulated and 292 downregulated genes) characterized the signature (Figure 3B). Functional analysis identified the cytokine-cytokine receptor interaction pathway as the most upregulated. Pathways related to T-cell differentiation, T-cell receptor signaling and primary immunodeficiency were the most downregulated (supplemental Table 6). Gene Set Enrichment Analysis showed that BCL11B targets were significantly deregulated in the signature of *BCL11B*-a AL cases (false discovery rate [FDR] = 0.07; Figure 3C). Although the analysis of differentially expressed genes revealed a marked skewness toward upregulation at the global level, the same analysis, focusing on BCL11B direct transcriptional targets, identified an opposite pattern, with a prevalent downregulation involving 107 of 179 (60%) known BCL11B target genes (Figure 3D). This result suggests that 14q32 translocations cause activation of the BCL11B transcriptional repressor program. Although RNA-seq confirmed the hyperexpression of *SPI1*/PU.1 in *BCL11B*-a AL compared with other leukemias,

Figure 4. Mutational profile of *BCL11B*-a AL. Oncoprint heat map showing all sequence variants detected in *BCL11B*-a AL cases. In addition to somatic mutations (dark green), variants in which the somatic or germline origin could not be definitively assessed (light green) are indicated. Additional gene alterations are represented by different colors. Mutational analysis was not performed in cases 15 and 19 because of lack of material. cnLOH, copy neutral loss of heterozygosity.

known target genes of PU.1 were not significantly enriched in *BCL11B*-a AL (data not shown).

Compared with the T-ALL series and with ETP-ALL cases as a separate group, *BCL11B*-a AL cases showed a significant upregulation: 6265 and 5787 genes, respectively (supplemental Figure 8A-B). Functional analysis showed that the cytokine-cytokine receptor interaction was the most upregulated pathway vs both T-ALL and ETP-ALL. It included positive regulators of JAK/STAT signaling, such as *IFNL1*, *IFNL3*, *IFNA*, *IL6*, *IL7*, *IL19*, *IL20*, *IL24*, *IL27*, *OSMR*, *IL13RA1*, and *PRLR* (supplemental Table 6).[24,25] A significant downregulation of 390 genes vs T-ALL and of 324 genes vs ETP-ALL was found (supplemental Figure 8A-B). Functional analysis identified hematopoietic cell lineage and T-cell receptor signaling as the most downregulated pathways (supplemental Table 6), suggesting that the T-lymphoid program is not yet fully activated in this immature entity. These pathways included genes encoding T-cell surface antigens (ie, *CD1A*, *CD1B*, *CD1E*, *CD3D*, *CD3E*, *CD3G*, *CD5*, *CD8A*, and *CD28*) and T-cell signaling molecules (*TCF7*, *LCK*, *RASGRP1*, *JUN*, and *RAG1*).

When compared with AML, *BCL11B*-a AL showed upregulation of 5118 genes and downregulation of 680 genes (supplemental Figure 8C). Ribosome biogenesis (including genes encoding ribosomal protein subunits) and protein translation pathways (ie, *EIF3CL* and *EIF4A1*) emerged as the most upregulated (supplemental Table 6).

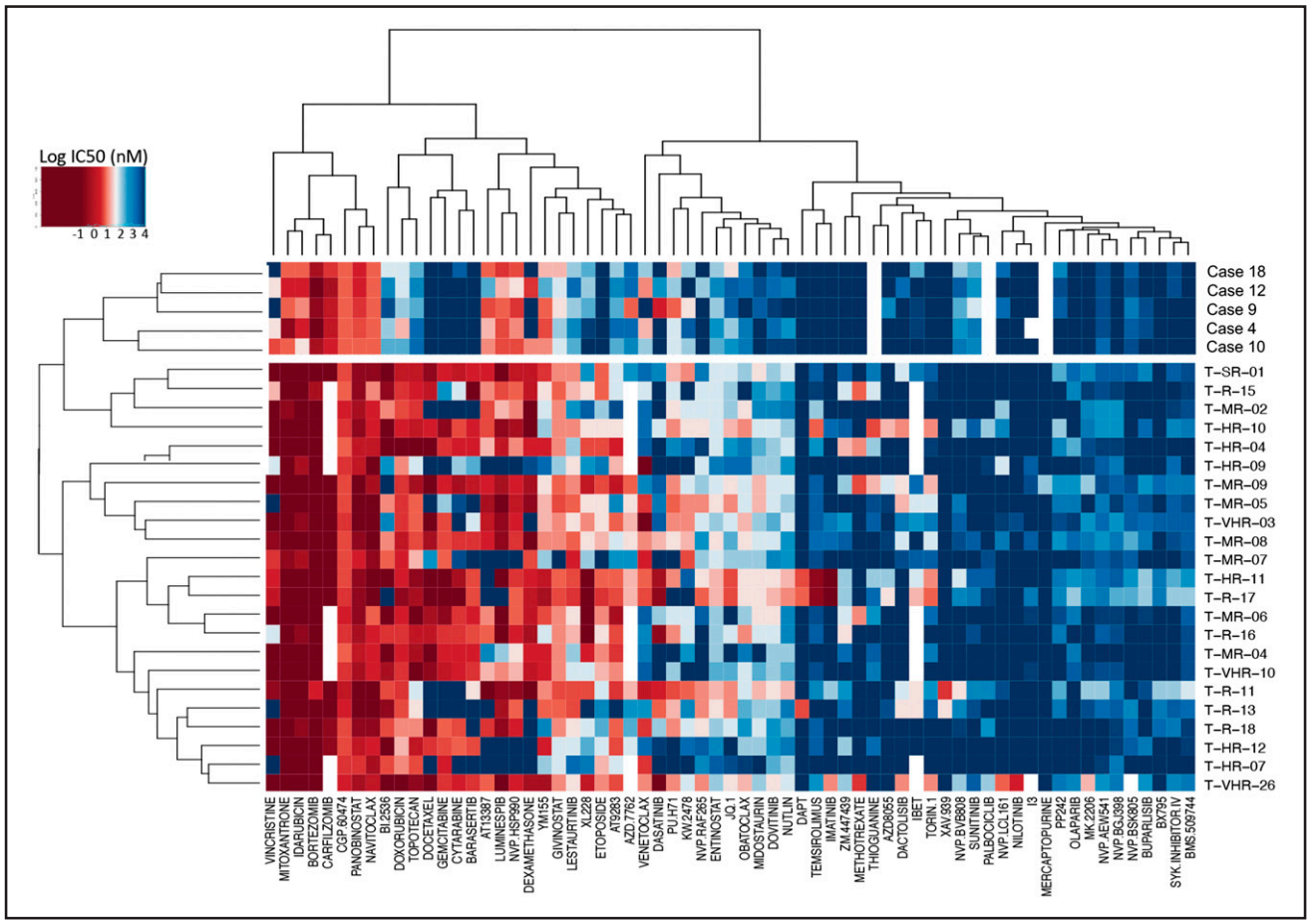

Figure 5. Drug response profile of *BCL11B*-a AL. Heat map indicating the response of *BCL11B*-a AL (5 cases: 4, 9, 10, 12, and 18) compared with T-ALL (23 cases)[17] to 65 compounds and represented by 50% inhibitory concentration values (IC_{50}). Samples (rows) are in order according to clinical classification (*BCL11B*-a AL and T-ALL), and compounds are reported in columns.

The mutational landscape of *BCL11B*-a acute leukemia

NGS revealed a burden of variants ranging from 2 to 13 per case (mean, 5.7 events). Overall, 95 variants were found in *BCL11B*-a AL cases (Figure 4), 29 of which are not reported in the main variant databases (ie, gnomAD, dbSNP, 1000 Genome Project, Clinvar, HGMD, Ensembl, or COSMIC). For each variant, the degree of pathogenicity is shown in supplemental Table 7 and the supplemental Material. All investigated cases had *FLT3* mutations, which comprised internal tandem duplication (ITD; n = 12), nucleotide substitution at the tyrosine-kinase domain (n = 4), or both (n = 1). No *NOTCH1 or FBXW7* mutations were detected in the *BCL11B*-a ALs tested (supplemental Material). However, a *NOTCH2* somatic mutation was found in ETP-ALL case 10 (supplemental Table 7). *RUNX1* mutations were present in 3 cases. A variety of epigenetic modulator genes (*WT1* [n = 8], *DNMT3A* [n = 6], *TET2* [n = 4], *EZH2*, *EP300*, and *ASXL2* [n = 2, each]) were affected in all but 1 case (Figure 4; supplemental Table 7). All other events involving epigenetic genes were not recurrent. In 3 cases, targeted sequencing on paired diagnosis-remission samples, showed that *DNMT3A* mutations remained present in hematological and cytogenetic remission (supplemental Table 8). Additional sporadic variants in genes involved in cell signaling, RNA processing, cell adhesion, cell cycle, and transcriptional regulation were also found (Figure 4; supplemental Table 7).

BCL11B-a ALs are sensitive to tyrosine kinase and JAK/STAT inhibitors

To detect functional vulnerabilities, we performed ex vivo drug response profiling in 5 cases with *BCL11B*-a AL cultured on human mesenchymal stromal cells. Comparing the specific drug sensitivities to an unrelated cohort of T-ALL cases,[17] in *BCL11B*-a AL cases, we found a striking decrease in activity for the genotoxic agents used in both AML and T-ALL, such as docetaxel, mitoxantrone, idarubicin, etoposide, doxorubicin, cytarabine, gemcitabine, and topotecan (Figure 5; supplemental Figure 9). Corroborating the genomic data, that suggest activated FLT3 and JAK/STAT pathways, we found higher sensitivity to tyrosine kinases (sunitinib, crenolanib) and JAK/STAT inhibitors (NVP-BVB808, momelotinib, fedratinib, and NVP-BSK805) in *BCL11B*-a AL cases compared with other T-ALL samples (Figure 5; supplemental Figure 9). Of note, the tyrosine kinase inhibitor midostaurin showed low activity in *BCL11B*-a AL cases, despite the presence of *FLT3* mutations, indicating that drug sensitivities may depend on more complex factors than candidate gene mutations (Figure 5; supplemental Figure 9).

Discussion

In this study, different types of leukemia, variably classified as immature AML, ETP-ALL, or T/M MPAL according to immunophenotype, converged into genetic disease characterized by 14q32 translocations activating *BCL11B*.

BCL11B is a C_2H_2 zinc-finger transcription factor also defined as a "guardian of T-cell fate"[26] for its role in the maintenance of T-cell identity.[10,11] In human T-ALL, it undergoes translocations that alternatively activate *TLX3*, *HOXA*, *NKX2-1*, and *NKX2-5* genes.[13,27-30] It may also act as a tumor suppressor undergoing loss-of-function mutations and deletions in 13% and 3% of T-ALL and ETP-ALL cases, respectively.[31] The physiological expression of *BCL11B* starts in the transition between the stages DN2a and DN2b of the thymocyte, and it is maintained along the entire lineage until reaching mature T cells.[11,32] High levels of *BCL11B* have been reported in T-cell leukemia/lymphoma (ATLL), T-ALL, and immature AML.[33-35]

In our FISH screening of malignant hemopathies, *BCL11B* was shown to be involved in known T-ALL translocations and in a subset of acute leukemias characterized by recombination of 14q32 with 4 alternative chromosomes partners: 2q22.3, 6q25.3, 7q21.2, and 8q24.2. Interestingly, for the last 3 regions, the full-length *BCL11B* translocated to regions without known genes and was likely activated by elements that were previously involved in oncogenesis: the superenhancer of *ARID1B* at 6q25.3[18,19,35]; a superenhancer located inside the *CDK6* gene, at 7q21.2[18,28]; and the BENC superenhancer at 8q24.2.[36,37] Rearrangements involving 2q22.3 as the chromosome partner, instead generated a *ZEB2-BCL11B* fusion gene that was highly expressed in the leukemic cells. As a member of the ZEB family, ZEB2 controls cellular motility, stem cell properties, apoptosis and senescence, and it is crucial for epithelial-mesenchymal transition.[38] Interestingly, both ZEB2 and BCL11B act as transcriptional repressors by interacting with the NuRD corepressor complex.[8,9,39,40] As in the fusion protein, ZEB2 maintains its NuRD interaction motif RRKQxxP at the N terminal and BCL11B maintains its C_2H_2-ZEB at the C terminal,[41] an effect of their chimeric product at the transcriptional level is plausible. In our study, we found high expression of both genes, not only in the leukemic bone marrow of cases bearing the fusion, but also in the other *BCL11B*-a AL cases. However, our results from individual longitudinal analyses pointed to *BCL11B* deregulation as the major pathogenetic event, as *BCL11B*, but not *ZEB2*, decreased at hematological and cytogenetic remission, as expected for clonal driver changes. Nevertheless, because the function of ZEB2 has been emphasized in both myeloid and ETP-ALL leukemogenesis,[22,23] a hypothetical role for *ZEB2* expression in the leukemic process of *BCL11B*-a AL should be further investigated.

To provide a diagnostic test to differentiate *BCL11B*-activating rearrangements from other typical T-ALL–associated translocations,[42] in which known oncogenes are activated by *BCL11B* downstream enhancer,[13,27-30] we set up a specific FISH assay that was useful for diagnosing the new *BCL11B*-a AL entity by discriminating the cluster of breakpoints at the *BCL11B*/14q32 that fall telomeric to the clusters of the other 14q32/*BCL11B* translocations that activate oncogenes.

The transcriptome profile grouped the variety of AL with *BCL11B* activation and identified a new entity in which the BCL11B driver effect was emphasized by the impact of its targets within the specific signature. A common phenotypic denominator of these leukemic blasts emerged, with expression of immature, myeloid, and T-lymphoid antigens, suggesting potential toward both lymphoid and myeloid programs in the leukemic progenitor. Interestingly, *SPI1*/PU.1 expression in the *BCL11B*-a AL signature was similar to that observed in AML, but was significantly higher than the level found in T-ALL. As *SPI1*/PU.1 is a well-characterized, double-faced T-lymphoid and myeloid differentiation player, depending on cell context and epigenetics,[43,44] it is a good candidate to support myeloid potential in *BCL11B*-a AL. A putative oncogenic role of *SPI1*/PU.1 in this leukemia subset is suggested by the occurrence of recurrent *SPI1*/PU.1 fusions in immature T-ALL.[43,45]

A focus on the mutational landscape showed that both *FLT3* and epigenetic genes were affected in the *BCL11B*-a AL cases. Interestingly, *WT1*, *DNMT3A*, and *TET2*, the most frequently mutated epigenetic genes in this study, have been reported in acute leukemia with expression of myeloid and/or T-lymphoid antigens.[46-48] Furthermore, the persistence of *DNMT3A* gene mutations at remission has been described in both AML[49] and T-ALL.[50] These findings suggest that *DNMT3A* mutations identify preleukemic clonal hematopoiesis underlying the development of different leukemia subtypes.[48] With respect to *FLT3* mutations, including the ITD and D835 variants, they did not discriminate immunological and cytogenetic leukemia subsets. However, they have been traced as important second hits, so-called class 2 mutations, supporting malignant proliferation.[48,51] Remarkably, an in vivo mouse model has shown that, when combined, *FLT3*-ITD and *DNMT3A* loss-of-function mutations recapitulated a variety of human leukemias, including mixed-lineage leukemia expressing both myeloid and T-cell markers.[52] Altogether, these findings suggest a 3-hit model in the pathogenesis of *BCL11B*-a AL, in which epigenetic event(s) may act by opening the chromatin in a totipotent progenitor, thus favoring *BCL11B* rearrangements; *FLT3* mutations behave as a crucial hit to support proliferation.[48]

Functional drug response further supported the specific biologic profile of *BCL11B*-a AL and provided some new insights. In addition to the poor sensitivity to genotoxic agents used in either AML or T-ALL induction therapy, a higher sensitivity to distinct tyrosine kinase and JAK/STAT pathway inhibitors emerged. Although the lack of sensitivity to genotoxic agents appeared not to be predicted by genomic lesions, they were instead in keeping with sensitivity to JAK/STAT and tyrosine kinase inhibition.

In summary, in this new leukemia entity, genomic findings overstep immunological classification of immature blasts, providing new insights for precise diagnosis and for tailored therapy in prospective clinical trials.

Acknowledgments

The authors thank Lucia Brandimarte for invaluable help during the development of this work.

C. Mecucci was supported by PRIN2017 (Ministero Italiano Università e Ricerca [MIUR]) code 2017PPS2X4. J.-P.B. and B.B. were supported by the Empiris Foundation.

Authorship

Contribution: C. Mecucci, R.L.S., V.P., S. Arniani, and M.M. performed and analyzed the cytogenetics, FISH, and SNPa; D.D.G., P.G., F.P., C. Matteucci, Z.K.A., K.D.K., S. Aerts, J.C., and R.P. performed and analyzed molecular and NGS studies; C. Mecucci, R.L.S., C.J.H., N.T., G.D.S., G.R., R.B., and P.V. collected samples and patient data; B.B. and J.-P.B. performed the drug profile; C. Mecucci conceived the study; and C. Mecucci, D.D.G., and R.L.S. collected all the data and wrote the manuscript.

Conflict-of-interest disclosure: The authors declare no competing financial interests.

ORCID profiles: Z.A.K., 0000-0003-4761-8169; K.D.K., 0000-0002-7420-9531; C. Matteucci, 0000-0002-9553-4819; P.V., 0000-0003-4719-1935; J.C., 0000-0001-6626-5843; R.P., 0000-0003-4198-9620; C. Mecucci, 0000-0002-1623-0148.

Correspondence: Cristina Mecucci, Hematology, University of Perugia, CREO, P.le Menghini 9, 06132 Perugia, Italy; e-mail: cristina.mecucci@unipg.it.

Footnote

Submitted 21 December 2020; accepted 23 March 2021; prepublished online on *Blood* First Edition 19 April 2021. DOI 10.1182/blood.2020010510.

*D.D.G. and R.L.S. contributed equally to this study.

The data reported in this article have been deposited in the National Center for Biotechnology Information, Gene Expression Omnibus (GEO) (accession numbers GSE162283, GSE162000 for SNParray, GSE162280 for RNA-Seq, and GSE162282 for sequencing data).

The online version of this article contains a data supplement.

There is a *Blood* Commentary on this article in this issue.

The publication costs of this article were defrayed in part by page charge payment. Therefore, and solely to indicate this fact, this article is hereby marked "advertisement" in accordance with 18 USC section 1734.

REFERENCES

1. Swerdlow SH, Campo E, Harris NL, et al. *WHO Classification of Tumours of Haematopoietic and Lymphoid Tissues*. 4th ed., revised. Lyon, France: World Health Organization; 2017.
2. Alexander TB, Gu Z, Iacobucci I, et al. The genetic basis and cell of origin of mixed phenotype acute leukaemia. *Nature*. 2018; 562(7727):373-379.
3. Takahashi K, Wang F, Morita K, et al. Integrative genomic analysis of adult mixed phenotype acute leukemia delineates lineage associated molecular subtypes. *Nat Commun*. 2018;9(1):2670.
4. Patrick K, Wade R, Goulden N, et al. Outcome for children and young people with Early T-cell precursor acute lymphoblastic leukaemia treated on a contemporary protocol, UKALL 2003. *Br J Haematol*. 2014; 166(3):421-424.
5. Conter V, Valsecchi MG, Buldini B, et al. Early T-cell precursor acute lymphoblastic leukaemia in children treated in AIEOP centres with AIEOP-BFM protocols: a retrospective analysis. *Lancet Haematol*. 2016; 3(2):e80-e86.
6. Coustan-Smith E, Mullighan CG, Onciu M, et al. Early T-cell precursor leukaemia: a subtype of very high-risk acute lymphoblastic leukaemia. *Lancet Oncol*. 2009; 10(2):147-156.
7. Zhang J, Ding L, Holmfeldt L, et al. The genetic basis of early T-cell precursor acute lymphoblastic leukaemia. *Nature*. 2012;481(7380):157-163.
8. Cismasiu VB, Adamo K, Gecewicz J, Duque J, Lin Q, Avram D. BCL11B functionally associates with the NuRD complex in T lymphocytes to repress targeted promoter. *Oncogene*. 2005;24(45):6753-6764.
9. Dubuissez M, Loison I, Paget S, et al. Protein kinase C–mediated phosphorylation of BCL11B at serine 2 negatively regulates Its interaction with NuRD complexes during CD4+ T-cell activation. *Mol Cell Biol*. 2016; 36(13):1881-1898.
10. Liu P, Li P, Burke S. Critical roles of Bcl11b in T-cell development and maintenance of T-cell identity. *Immunol Rev*. 2010;238(1): 138-149.
11. Rothenberg EV. Programming for T-lymphocyte fates: modularity and mechanisms. *Genes Dev*. 2019;33(17-18):1117-1135.
12. Ley TJ, Miller C, Ding L, et al; Cancer Genome Atlas Research Network. Genomic and epigenomic landscapes of adult de novo acute myeloid leukemia. *N Engl J Med*. 2013;368(22):2059-2074.
13. Liu Y, Easton J, Shao Y, et al. The genomic landscape of pediatric and young adult T-lineage acute lymphoblastic leukemia. *Nat Genet*. 2017;49(8):1211-1218.
14. Cerami E, Gao J, Dogrusoz U, et al. The cBio cancer genomics portal: an open platform for exploring multidimensional cancer genomics data. *Cancer Discov*. 2012;2(5): 401-404.
15. Gao J, Aksoy BA, Dogrusoz U, et al. Integrative analysis of complex cancer genomics and clinical profiles using the cBioPortal. *Sci Signal*. 2013;6(269):pl1.
16. Grossman RL, Heath AP, Ferretti V, et al. Toward a Shared Vision for Cancer Genomic Data. *N Engl J Med*. 2016;375(12): 1109-1112.
17. Frismantas V, Dobay MP, Rinaldi A, et al. Ex vivo drug response profiling detects recurrent sensitivity patterns in drug-resistant acute lymphoblastic leukemia. *Blood*. 2017;129(11):e26-e37.
18. Hnisz D, Abraham BJ, Lee TI, et al. Super-enhancers in the control of cell identity and disease. *Cell*. 2013;155(4):934-947.
19. Wang W, Beird H, Kroll CJ, et al. T(6;14)(q25;q32) involves BCL11B and is highly associated with mixed-phenotype acute leukemia, T/myeloid. *Leukemia*. 2020;34(9):2509-2512.
20. La Starza R, Barba G, Demeyer S, et al. Deletions of the long arm of chromosome 5 define subgroups of T-cell acute lymphoblastic leukemia. *Haematologica*. 2016;101(8):951-958.
21. Rothenberg EV, Hosokawa H, Ungerbäck J. Mechanisms of Action of Hematopoietic Transcription Factor PU.1 in Initiation of T-Cell Development. *Front Immunol*. 2019; 10:228.
22. Goossens S, Radaelli E, Blanchet O, et al. ZEB2 drives immature T-cell lymphoblastic leukaemia development via enhanced tumour-initiating potential and IL-7 receptor signalling. *Nat Commun*. 2015;6(1):5794.
23. Li J, Riedt T, Goossens S, et al. The EMT transcription factor Zeb2 controls adult murine hematopoietic differentiation by regulating cytokine signaling. *Blood*. 2017;129(4):460-472.
24. Baker SJ, Rane SG, Reddy EP. Hematopoietic cytokine receptor signaling. *Oncogene*. 2007; 26(47):6724-6737.
25. Hammarén HM, Virtanen AT, Raivola J, Silvennoinen O. The regulation of JAKs in cytokine signaling and its breakdown in disease. *Cytokine*. 2019;118:48-63.
26. Di Santo JP. Immunology. A guardian of T cell fate. *Science*. 2010;329(5987):44-45.
27. Nagel S, Kaufmann M, Drexler HG, MacLeod RAF. The cardiac homeobox gene NKX2-5 is deregulated by juxtaposition with BCL11B in pediatric T-ALL cell lines via a novel t(5;14)(q35.1;q32.2). *Cancer Res*. 2003;63(17): 5329-5334.
28. Su XY, Busson M, Della Valle V, et al. Various types of rearrangements target TLX3 locus in T-cell acute lymphoblastic leukemia. *Genes Chromosomes Cancer*. 2004;41(3):243-249.
29. Su X, Drabkin H, Clappier E, et al. Transforming potential of the T-cell acute lymphoblastic leukemia-associated homeobox genes HOXA13, TLX1, and TLX3. *Genes Chromosomes Cancer*. 2006;45(9):846-855.
30. Nagel S, Scherr M, Kel A, et al. Activation of TLX3 and NKX2-5 in t(5;14)(q35;q32) T-cell

acute lymphoblastic leukemia by remote 3'-BCL11B enhancers and coregulation by PU.1 and HMGA1. *Cancer Res.* 2007;67(4):1461-1471.

31. De Keersmaecker K, Real PJ, Gatta GD, et al. The TLX1 oncogene drives aneuploidy in T cell transformation. *Nat Med.* 2010; 16(11):1321-1327.

32. Kadoch C, Hargreaves DC, Hodges C, et al. Proteomic and bioinformatic analysis of mammalian SWI/SNF complexes identifies extensive roles in human malignancy. *Nat Genet.* 2013;45(6):592-601.

33. Oshiro A, Tagawa H, Ohshima K, et al. Identification of subtype-specific genomic alterations in aggressive adult T-cell leukemia/lymphoma. *Blood.* 2006;107(11):4500-4507.

34. Przybylski GK, Dik WA, Wanzeck J, et al. Disruption of the BCL11B gene through inv(14)(q11.2q32.31) results in the expression of BCL11B-TRDC fusion transcripts and is associated with the absence of wild-type BCL11B transcripts in T-ALL. *Leukemia.* 2005;19(2):201-208.

35. Abbas S, Sanders MA, Zeilemaker A, et al. Integrated genome-wide genotyping and gene expression profiling reveals BCL11B as a putative oncogene in acute myeloid leukemia with 14q32 aberrations. *Haematologica.* 2014;99(5):848-857.

36. Lovén J, Hoke HA, Lin CY, et al. Selective inhibition of tumor oncogenes by disruption of super-enhancers. *Cell.* 2013; 153(2):320-334.

37. Bahr C, von Paleske L, Uslu VV, et al. A Myc enhancer cluster regulates normal and leukaemic haematopoietic stem cell hierarchies [published correction appears in *Nature.* 2018;558(7711):E4]. *Nature.* 2018; 553(7689):515-520.

38. Lamouille S, Xu J, Derynck R. Molecular mechanisms of epithelial-mesenchymal transition. *Nat Rev Mol Cell Biol.* 2014; 15(3):178-196.

39. Verstappen G, van Grunsven LA, Michiels C, et al. Atypical Mowat-Wilson patient confirms the importance of the novel association between ZFHX1B/SIP1 and NuRD corepressor complex. *Hum Mol Genet.* 2008;17(8):1175-1183.

40. Si W, Huang W, Zheng Y, et al. Dysfunction of the reciprocal feedback loop between GATA3- and ZEB2-nucleated repression programs contributes to breast cancer metastasis. *Cancer Cell.* 2015;27(6):822-836.

41. Avram D, Fields A, Pretty On Top K, Nevrivy DJ, Ishmael JE, Leid M. Isolation of a novel family of C(2)H(2) zinc finger proteins implicated in transcriptional repression mediated by chicken ovalbumin upstream promoter transcription factor (COUP-TF) orphan nuclear receptors. *J Biol Chem.* 2000;275(14):10315-10322.

42. La Starza R, Pierini V, Pierini T, et al. Design of a comprehensive fluorescence in situ hybridization assay for genetic classification of T-cell acute lymphoblastic leukemia. *J Mol Diagn.* 2020;22(5):629-639.

43. Homminga I, Pieters R, Langerak AW, et al. Integrated transcript and genome analyses reveal NKX2-1 and MEF2C as potential oncogenes in T cell acute lymphoblastic leukemia. *Cancer Cell.* 2011;19(4):484-497.

44. Pundhir S, Bratt Lauridsen FK, Schuster MB, et al. Enhancer and transcription factor dynamics during myeloid differentiation reveal an early differentiation block in Cebpa null progenitors. *Cell Rep.* 2018;23(9):2744-2757.

45. Seki M, Kimura S, Isobe T, et al. Recurrent SPI1 (PU.1) fusions in high-risk pediatric T cell acute lymphoblastic leukemia. *Nat Genet.* 2017;49(8):1274-1281.

46. Peirs S, Van der Meulen J, Van de Walle I, et al. Epigenetics in T-cell acute lymphoblastic leukemia. *Immunol Rev.* 2015;263(1):50-67.

47. Pronier E, Bowman RL, Ahn J, et al. Genetic and epigenetic evolution as a contributor to WT1-mutant leukemogenesis. *Blood.* 2018;132(12): 1265-1278.

48. Shlush LI, Zandi S, Mitchell A, et al; HALT Pan-Leukemia Gene Panel Consortium. Identification of pre-leukaemic haematopoietic stem cells in acute leukaemia [published correction appears in *Nature.* 2014;508(7496):420]. *Nature.* 2014; 506(7488):328-333.

49. Gaidzik VI, Weber D, Paschka P, et al; German-Austrian Acute Myeloid Leukemia Study Group (AMLSG). DNMT3A mutant transcript levels persist in remission and do not predict outcome in patients with acute myeloid leukemia. *Leukemia.* 2018;32(1):30-37.

50. Bond J, Touzart A, Leprêtre S, et al. *DNMT3A* mutation is associated with increased age and adverse outcome in adult T-cell acute lymphoblastic leukemia. *Haematologica.* 2019;104(8): 1617-1625.

51. Gilliland DG, Griffin JD. The roles of FLT3 in hematopoiesis and leukemia. *Blood.* 2002;100(5): 1532-1542.

52. Yang L, Rodriguez B, Mayle A, et al. DNMT3A Loss drives enhancer hypomethylation in FLT3-ITD-associated leukemias [published correction appears in *Cancer Cell.* 2016;30(2):363–365]. *Cancer Cell.* 2016;29(6):922-934.